

Adaptive Detection of On-Orbit Jamming for Securing GEO Satellite Links

Anouar Boumeftah*, Olfa Ben Yahia*, Jean-François Frigon*, Gregory Falco†, Gunes Karabulut Kurt*

* Poly-Grames Research Center, Department of Electrical Engineering, Polytechnique Montréal, Montréal, QC, Canada

† Cornell University Ithaca, NY, US

{anouar.boumeftah, olfa.ben-yahia, j-f.frigon, gunes.kurt}@polymtl.ca, gfalco@cornell.edu

Abstract—This paper introduces a scenario where a maneuverable satellite in geostationary orbit (GEO) conducts on-orbit attacks, targeting communication between a GEO satellite and a ground station, with the ability to switch between stationary and time-variant jamming modes. We propose a machine learning-based detection approach, employing the random forest algorithm with principal component analysis (PCA) to enhance detection accuracy in the stationary model. At the same time, an adaptive threshold-based technique is implemented for the time-variant model to detect dynamic jamming events effectively. Our methodology emphasizes the need for the use of orbital dynamics in integrating physical constraints from satellite dynamics to improve model robustness and detection accuracy. Simulation results highlight the effectiveness of PCA in enhancing the performance of the stationary model, while the adaptive thresholding method achieves high accuracy in detecting jamming in the time-variant scenario. This approach provides a robust solution for mitigating the evolving threats to satellite communication in GEO environments.

Index Terms—Geostationary orbit (GEO), on-orbit jamming, machine learning in satellite security, satellite communication security, time-variant jamming, satellite interference mitigation.

I. INTRODUCTION

Satellites play an increasingly critical role in future communication networks by enabling connectivity in areas where terrestrial networks face challenges in providing continuous service. Recent advancements in satellite systems have attracted significant attention, primarily due to their extensive geographic reach and flexible deployment, making them a promising solution for global communications. These developments are transforming traditional communication methods by improving the effectiveness of emergency monitoring through space information networks [1]. With such networks, events on the opposite side of the Earth can be detected and transmitted to ground stations anywhere, enhancing disaster prevention, relief efforts, and emergency response capabilities.

As space information networks become crucial to civilian and military operations, their role extends to global positioning, navigation, and space tracking. This growing reliance on satellite-based systems brings increasing security demands, particularly in ensuring the resilience of critical infrastructure. Geostationary orbit (GEO) satellites, in particular, are essential for maintaining continuous coverage and delivering uninterrupted services, making them key targets for various threats, including eavesdropping, spoofing, and jamming attacks [2].

Therefore, understanding and addressing these vulnerabilities is vital to secure satellite networks (SatNets).

The existing literature primarily studies active and passive attacks in the context of ground stations, with a limited focus on space-based threats. However, concerns have grown following real-world incidents, such as the 2022 cyberattack on Viasat’s KA-SAT network during the Ukraine conflict, which disrupted military and civilian communications across Europe [3]. Currently, jamming poses a critical threat to satellite links, particularly in satellite-to-ground and ground-to-satellite communications. Most anti-jamming strategies have focused on these links to ensure the availability of satellite services. In contrast, the satellite-to-satellite link has received less attention due to the challenges of jamming at large distances. Recent studies, however, have begun exploring security solutions for various space environments. For instance, a non-cooperative jamming effect on inter-satellite link (ISL) rates in mega-constellations has been studied in [4]. By defining the main jamming region and analyzing factors like jamming power, constellation scale, and inclination, the study provides insights into the optimal conditions for jamming efficiency. The results show that close constellation inclinations maximize jamming effects. Similarly, a location-based authentication framework has been proposed for secure communication in cislunar space, utilizing distance verification and adaptive decision criteria to enhance link reliability [5]. These studies highlight the diverse security challenges across different space missions.

In the current literature, jamming detection methods are broadly categorized into two classes: non-machine learning-based approaches [6]–[9] and machine learning-based methods [10]–[14]. For instance, [6] introduces a secure architecture for space information networks, incorporating beam hopping and relay selection to protect against uplink jamming and downlink eavesdropping. In [7], the feasibility of reactive jamming in satellites is analyzed, and a mitigation strategy is proposed, leveraging coding and interleaving schemes that exploit geometric constraints to reduce the impact of reactive jammers. The work in [8] addresses camouflage jamming in satellite Internet of Things networks, introducing detection methods that demonstrate the effectiveness of a simple counting technique for identifying jamming attempts while also highlighting system vulnerabilities. Meanwhile, [9] explores the feasibility of integrating an orbital intrusion prevention system to protect LEO satellites from malicious ground station transmissions,

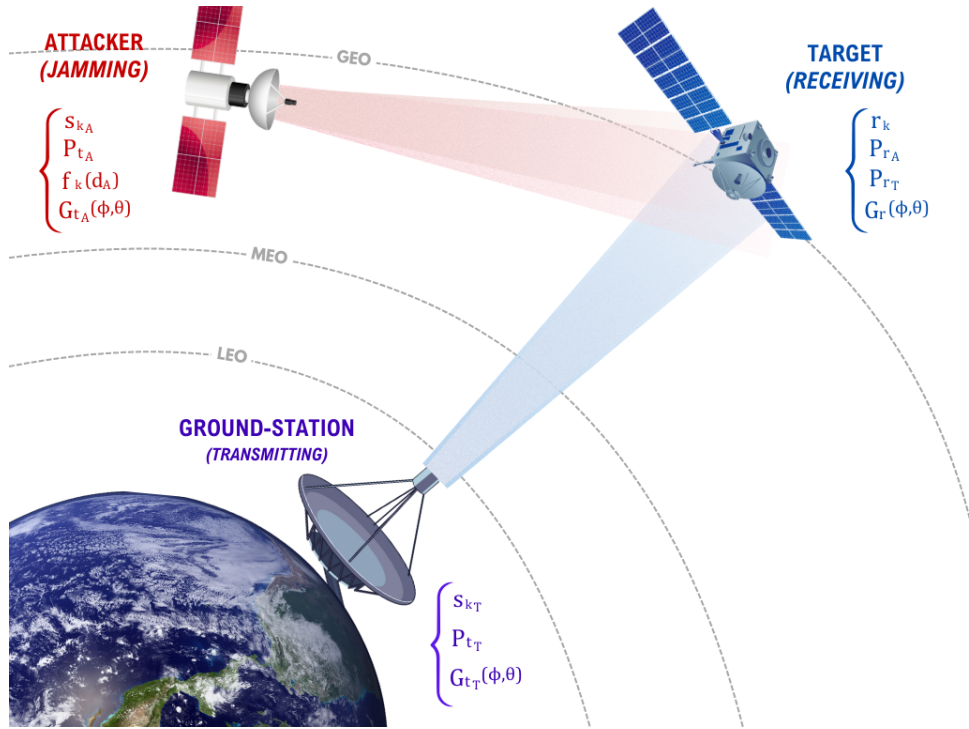


Fig. 1: System model illustration: satellite-to-satellite uplink jamming in GEO

demonstrating the potential of selective jamming through real-life scenario simulations and emphasizing the need for on-orbit security measures.

While non-learning-based methods can be effective in specific scenarios, they become less reliable when dealing with advanced intelligent jammers who can adapt and change their strategies through interaction. As a response, the introduction of artificial intelligence (AI) and machine learning (ML)-based approaches have emerged as robust solutions in detecting and countering such dynamic jamming threats, as these intelligent techniques can adapt to the evolving behavior of attackers, significantly enhancing the resilience and reliability of SatNets [10]. In this context, [11] demonstrates the value of ML-based jamming optimization in LEO satellites, leveraging a genetic algorithm for enhanced security against unauthorized broadcasts, while [12] underscores the advantages of using random forest, SVM, and neural networks in wireless networks for precise and cost-effective jamming detection. In addition, ML approaches have shown promise in detecting spoofing and jamming attacks for GPS and aerial platforms [13], [14].

While jamming has been extensively studied, most existing research primarily addresses ground-based jammers, with limited focus on space-based jamming threats. This leaves a significant gap, especially regarding attacks in GEO. Furthermore, current studies typically assume a stationary jamming model, where the attacker remains in a fixed position, neglecting the complexities of time-variant jamming models, where the attacker follows a specific trajectory over time. Motivated by these gaps, this paper addresses the emerging threats posed by satellite-to-satellite attacks in GEO, where

a GEO attacker jams the uplink communication between a ground station and a GEO satellite, as shown in Fig. 1. We focus specifically on both stationary and time-variant jamming scenarios. We propose a simulation framework and tailored detection methodologies to identify and mitigate these threats. The key contributions of our work are summarized as follows:

- We identify and contextualize on-orbit jamming threats in GEO, illustrating vulnerabilities arising from proximity-based attacks by maneuverable satellites that can engage in both passive and active jamming. This highlights the necessity of robust on-orbit detection mechanisms.
- We develop a comprehensive simulation framework for modeling stationary and time-variant jamming attacks in GEO. Using the systems tool kit (STK), we generate realistic satellite trajectories and communication parameters, including signal-to-noise ratio (SNR) and signal-to-jamming-and-noise ratio (SJNR), providing an adaptable tool for future studies in satellite security.
- We propose scenario-specific detection approaches, employing principal component analysis (PCA)-augmented random forest for stationary jamming scenarios and an adaptive threshold-based method for time-variant attacks. Our methodology incorporates orbital dynamics leveraging satellite dynamics to enhance the accuracy and robustness of jamming detection in GEO environments.

The remainder of the paper is organized as follows: Section II introduces a case study on anomalous proximity maneuvers by a geostationary satellite, highlighting risks associated with proximity-based threats in GEO. Section III details the

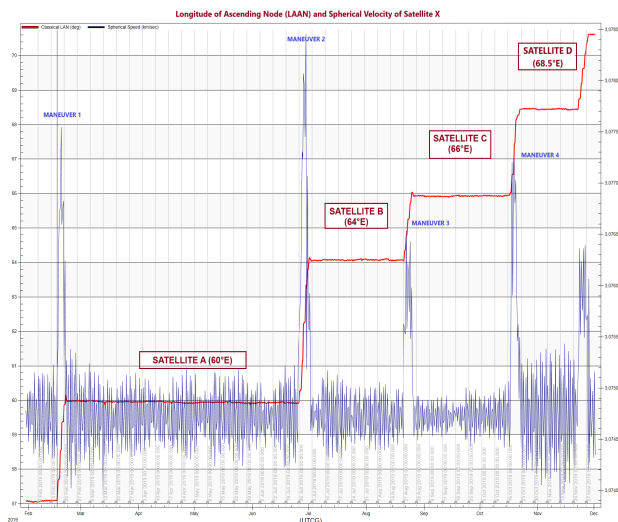


Fig. 2: Orbital maneuver patterns of satellite X: longitude of ascending node and spherical speed over time using STK

channels and the proposed system model. Section IV details the proposed method for stationary and time-variant jamming scenarios. Numerical results are discussed in Section V. Finally, Section VI concludes the paper.

II. CASE STUDY: ANOMALOUS PROXIMITY MANEUVERS BY A GEOSTATIONARY SATELLITE

In recent years, the security of geostationary communication satellites has faced increased concern, mainly due to the potential threats associated with maneuverable satellites performing frequent proximity operations. While much of the existing literature focuses on jamming and spoofing in ground-to-satellite, possible attacks involving proximity operations in GEO remain underexplored. To address this, we present a case study on a fictional satellite, designated as Satellite X, which exhibits highly atypical behavior by repeatedly maneuvering close to other GEO satellites, labeled as Satellites A, B, C, and D. This behavior highlights the potential risks of proximity-based interference or surveillance in GEO, emphasizing the importance of developing detection and mitigation strategies for such space-based threats.

a) Anomalous Maneuvering Patterns: In this scenario, we assume that Satellite X regularly adjusts its position through intentional orbital maneuvers. Unlike typical GEO satellites, which generally maintain fixed longitudes, Satellite X periodically maneuvers, pausing near specific locations before initiating another adjustment. This pattern of frequent repositioning deviates notably from standard GEO satellite operations, which aim to maintain a stable orbit with minimal adjustments. Additionally, Satellite X is observed to position itself near the locations of communication satellites A, B, C, and D.

b) Visualizing the Maneuvers and Orbital Data: To illustrate this behavior, Fig. 2 depicts a graph tracking the longitude of the ascending node (LAAN) and spherical speed

of Satellite X over time. In this figure, each abrupt change in LAAN and speed indicates a maneuver, followed by a period where Satellite X remains stationary near the position of one of the communication satellites, frequently aligning with Satellites A, B, C, or D. This pattern of approach-and-hold suggests an intentional strategy of positioning Satellite X near critical communication assets. Such a frequent sequence of maneuvers is highly atypical for a satellite in GEO, where fuel efficiency and orbital stability are primary operational goals. The repeated adjustments imply a strategic intention, potentially increasing the risk of eavesdropping, signal interception, or jamming for the targeted communication satellites.

c) Challenges and Importance of Dynamic Detection:

The dynamic nature of Satellite X’s maneuvering presents unique interference detection and mitigation challenges. Traditional detection models, often optimized for static interference sources, may fail to accurately identify jamming or interception attempts stemming from a moving source. In this case study, Satellite X’s proximity to Satellites A, B, C, and D and its repeated approach-and-hold maneuvers highlight the need for a time-variant detection model capable of responding to the satellite’s dynamic behavior.

III. CHANNELS AND SYSTEM MODEL

A. System Model

This paper introduces a novel scenario of on-orbit attacks in GEO. As illustrated in Fig. 1, the system model comprises a legitimate GEO satellite and an attacker operating in the same orbit. The legitimate satellite communicates with a ground station on Earth, while the attacker functions in two distinct modes: passive and active. The attacker transmits jamming signals toward the legitimate satellite and may operate stationary or time-variant. In the stationary approach, the attacker remains fixed at a particular location. In contrast, in the time-variant approach, the attacker adjusts its trajectory over time to maximize jamming impact while minimizing detection risk. Unlike the stationary jamming model commonly assumed in current studies, this dynamic time-variant approach—where the attacker alternates between different positions—introduces significant complexities for detection and mitigation.

For the uplink, given the significant distance between the ground station and the GEO satellite, coupled with the ground station’s limited transmission power, the transmitted data packets are more vulnerable to jamming attacks from an adversary. This risk becomes more prominent when the ground station employs basic or weak encryption. In the downlink, an attacker can intercept the communication due to the broadcast characteristics of satellite channels, posing potential threats to data security and privacy. In the literature, downlink jamming is considered less frequent because it is assumed that a jammer requires a direct line-of-sight (LOS) to the ground station to generate significant jamming power at the receiver’s input [15]. Uplink jamming relies heavily on obtaining detailed information about the target signal and requires considerable transmitter power to interfere with the satellite’s radio receivers, including sensors and command systems. Although

more challenging to execute, uplink jamming can have far-reaching consequences, potentially disrupting the satellite's service globally for all users [16]. While uplink jamming in the literature typically assumes a ground-based attacker, our model considers an attacker in GEO, thus representing an on-orbit uplink jamming scenario.

B. Communication Model

In the proposed model, the received signal at the legitimate satellite is modeled as a combination of the transmitted signal, path loss effects, noise introduced during transmission, and interference introduced during jamming. This is expressed mathematically for each sample k as:

$$r_k = \frac{s_{T,k}}{\sqrt{\text{loss}_T}} + n_k + \frac{f_k \cdot s_{A,k}}{\sqrt{\text{loss}_A}}, \quad (1)$$

where r_k represents the k th received signal sample at the legitimate satellite at time t , while $s_{T,k}$ denotes the k th transmitted modulated signal sample from the ground station. Similarly, $s_{A,k}$ indicates the k th transmitted signal sample from the attacker's transmitter. The noise at the k th sample, n_k , follows a complex normal distribution, denoted as $n_k \sim \mathcal{CN}(0, \sigma_{\text{noise}}^2)$. The term loss refers to the free space path loss (FSPL), which affects signal propagation. The indicator function f_k takes the value of 1 when jamming is present at sample k and 0 otherwise, as shown in the following expression:

$$f_k = \begin{cases} 1 & \text{if jamming is present at sample } k \\ 0 & \text{otherwise.} \end{cases}$$

The average transmitted power of the ground station, P_t , and the jammer, P_j , are determined by the expected values of the squared magnitudes of their transmitted signal samples, $s_{T,k}$ and $s_{A,k}$, respectively. These relationships are mathematically represented as follows:

$$P_t^{\text{avg}} = \mathbb{E} [|s_{T,k}|^2], \quad P_j^{\text{avg}} = \mathbb{E} [|s_{A,k}|^2]. \quad (2)$$

Similarly, the received signal strength (RSS) is calculated from the received signal samples r_k by averaging the squared magnitude of each sample, which can be expressed as:

$$\text{RSS} = \frac{1}{N} \sum_{k=1}^N |r_k|^2, \quad (3)$$

where N is the total number of samples.

IV. PROPOSED METHODOLOGY

This section outlines the scenario and data generation methodology for the proposed stationary and time-variant models.

A. Stationary Model

In this subsection, we describe the orbital dynamics and spatial configuration underlying the stationary simulation based on the system model shown in Fig. 1. This simulation evaluates the target satellite's vulnerability to jamming by examining various fixed positions the attacker might occupy within a defined volume of interest (VOI).

The ground station maintains a direct LOS with the target satellite, positioned directly beneath it on Earth's surface. Due to the orbit's geostationary nature, the target satellite remains stationary relative to the ground station, ensuring a stable communication link. The attacker, also in a GEO position, is a potential threat to this communication link. Possible attacker positions are generated within a predefined VOI surrounding the target satellite to simulate multiple jamming scenarios. The VOI is represented as a spherical region centered on the target satellite, with a radius R_{VOI} , establishing the spatial domain within which the attacker can maneuver. The spherical constraint for the attacker's position is defined as:

$$\|\mathbf{r}_A^{(i)} - \mathbf{r}_T\| \leq R_{\text{VOI}}, \quad (4)$$

where $\mathbf{r}_A^{(i)}$ represents the i -th position of the attacker within the VOI, \mathbf{r}_T denotes the fixed position of the target satellite in the geocentric coordinate system, and R_{VOI} is the VOI radius, set to a value such as 5,000 km to cover a significant critical area around the target satellite. Each attacker position $\mathbf{r}_A^{(i)}$ within the VOI is sampled uniformly to simulate various jamming scenarios. By generating multiple attacker positions within the VOI, we create a range of locations, each representing a distinct potential jamming scenario. Given that the target and attacker satellites are in GEO, their relative position remains fixed unless the attacker executes deliberate maneuvers. This stationary assumption simplifies the orbital dynamics, allowing the analysis to concentrate on intentional jamming tactics rather than accounting for orbital perturbations.

B. Time-Variant Model

This subsection introduces a time-variant approach for detecting satellite-to-satellite jamming in scenarios where the attacker is in motion relative to a stationary target satellite in a GEO.

a) Implementation and expected impact: Unlike the stationary approach, where the attacker's position is fixed, and a binary classifier detects potential threats at a set time t , the time-variant model dynamically adjusts detection thresholds based on transient signal variations, enhancing responsiveness to non-static conditions. The relative movement of an attacking satellite along its orbit introduces temporal changes in the signal characteristics received by the target. The time-variant model accounts for these fluctuations by recalculating adaptive thresholds and tracking the rate of change in crucial signal features. This adaptability improves the model's ability to detect transient jamming events, maintaining accuracy across various attack trajectories.

To generate trajectory data for the time-variant jamming detection study, we utilize the Systems Tool Kit (STK) software, which is interfacing with its programming API to automate satellite trajectory creation. Multiple trajectories are simulated through the STK scripting interface, each representing a unique "attacking" satellite in motion relative to a target satellite fixed in GEO. The process begins by initializing the STK environment and defining the target satellite's fixed position above a ground station. For each simulation, a unique attacker

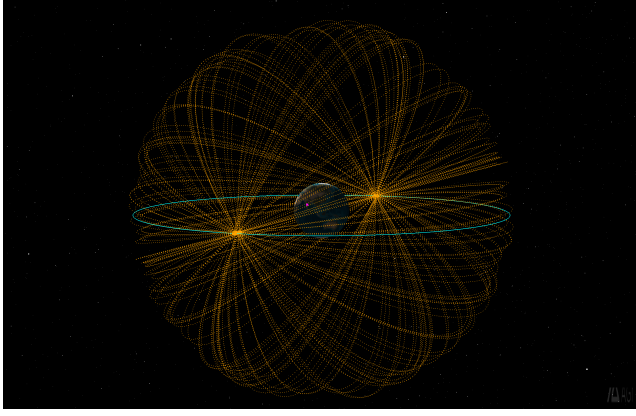


Fig. 3: Orbital visualization of the 100 automatically generated trajectories via STK Engine

satellite is instantiated with randomized orbital parameters, including semi-major axis and inclination, within the region of interest, as defined in the constraint (4). Each attacker's trajectory is generated by propagating its orbit, after which access intervals between the attacker and target satellites are calculated. During each access interval, range data—indicating the relative distance between the target and attacker—is obtained from the AER (Azimuth, Elevation, Range) report. As an initial approach to the time-variant model, this study considers only the range data, excluding factors such as attitude, line of sight, antenna pointing, azimuth, and elevation.

For the time-variant model, Fig. 3 displays the positions of 100 attacker satellites within a specific area around Earth, allowing us to see how close and clustered they are relative to the target. Closer and denser groups of attackers pose a higher risk for effective jamming. Fig. 4 illustrates the direct LOS connections (access links) between the attacker satellites and the target, showing which attackers have a clear path to interfere with the target. By examining these connections and measuring signal metrics like SJNR and RSS, we can identify which attacker positions are most likely to disrupt the target satellite's communication. This analysis helps identify high-risk positions within the VOI where jamming effects pose the most significant impact.

In addition, we calculate signal and power parameters at each epoch within the access interval to simulate communication and jamming interactions. This includes modeling the communication link between the ground station and the target satellite and the link between the attacker and the target. This allows the measurement of critical metrics such as received power, SNR, and SJNR. Periodic jamming events are simulated at specific epochs, labeling data points as "jammed" or "non-jammed." All resulting trajectory and communication data are stored in CSV files for subsequent analysis.

b) Adaptive thresholding approach: We consider adaptive thresholds and rate-of-change metrics to detect jamming events in the time-variant model, recalculated within a moving window. The key steps of the detection method are outlined as follows:

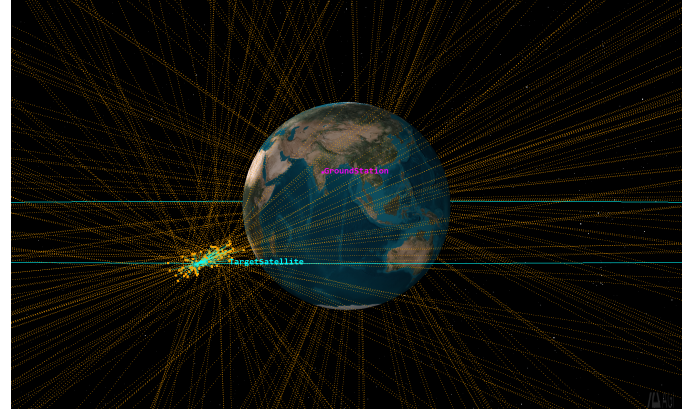


Fig. 4: Visualization of the 100 access links of the VOI-constrained attackers generated via STK Engine

- 1) Data processing across multiple trajectories: each trajectory file represents a unique relative path the attacking satellite takes concerning the target. We analyze signal features such as SJNR and total RSS for each trajectory to identify potential jamming events.
- 2) Dynamic thresholds calculation: adaptive thresholds are determined for each time step t using a moving window of size W . Within this window, the mean μ and standard deviation σ of each feature are computed. Two key parameters, α and β , are used to adjust the sensitivity for thresholding and rate-of-change detection.
 - α , the threshold multiplier, adjusts the sensitivity of each feature's threshold by scaling with the standard deviation. A higher α value decreases sensitivity to fluctuations, while a lower α increases sensitivity to signal changes.
 - β , the rate-of-change threshold, is used to detect abrupt deviations in feature values. This parameter sets the threshold for the rate of change in features such as SJNR and RSS between consecutive time steps, marking significant variations as potential jamming indicators.

The adaptive thresholds for SJNR and total RSS are calculated as follows:

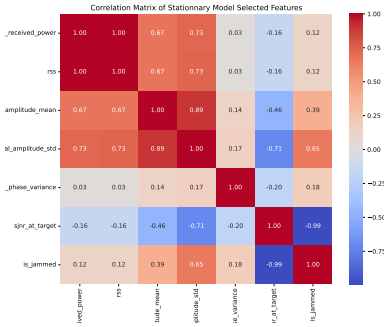
$$\text{Threshold}_{\text{SJNR}}(k) = \mu_{\text{SJNR}}(k) - \alpha \cdot \sigma_{\text{SJNR}}(k), \quad (5)$$

$$\text{Threshold}_{\text{RSS}}(k) = \mu_{\text{RSS}}(k) + \alpha \cdot \sigma_{\text{RSS}}(k), \quad (6)$$

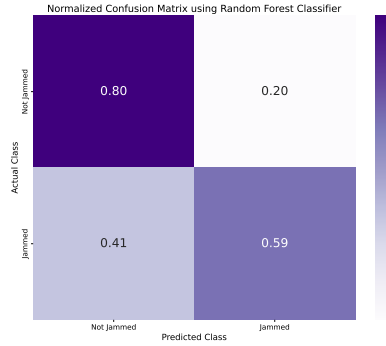
where $\mu_{\text{SJNR}}(k)$ and $\sigma_{\text{SJNR}}(k)$ represent the mean and standard deviation of the respective signal feature over the moving window of size W at sample index k .

- 3) Rate of change analysis: To detect abrupt changes in signal characteristics caused by the attacker's movement, we calculate the rate of change for SJNR and RSS between consecutive samples $k-1$ and k . This approach identifies significant shifts, which may indicate jamming activity. The rate of change for SJNR and RSS are given as follows:

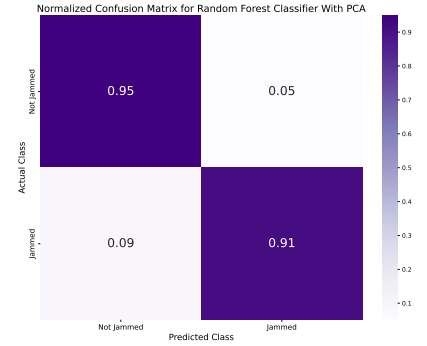
$$\Delta_{\text{SJNR}}(k) = |\text{SJNR}(k) - \text{SJNR}(k-1)|, \quad (7)$$



(a) Feature selection on signal metrics using correlation matrix



(b) Confusion matrix without PCA



(c) Confusion matrix with PCA

Fig. 5: Comparative analysis of feature correlation and performance for the stationary model. (a) Shows the correlation matrix for feature selection, indicating relationships and potential redundancies among features. (b) and (c) display confusion matrices for the random forest model without and with PCA, respectively, demonstrating improved classification accuracy with PCA applied.

$$\Delta_{RSS}(k) = |RSS(k) - RSS(k - 1)|. \quad (8)$$

4) Jamming detection criteria: At each sample k , the following detection conditions are evaluated:

- **Threshold condition:** A jamming event is flagged if any of the following inequalities hold:

$$SJNR(k) < \text{Threshold}_{SJNR}(k), \quad (9)$$

$$RSS(k) > \text{Threshold}_{RSS}(k). \quad (10)$$

- **Rate-of-change condition:** A jamming event is flagged if either of the following conditions holds:

$$\Delta_{SJNR}(k) > \beta \quad \text{or} \quad \Delta_{RSS}(k) > \beta. \quad (11)$$

The communication is labeled as "jammed" if one of the above conditions is satisfied.

V. NUMERICAL RESULTS AND DISCUSSION

This section outlines the performance metrics used for the system's evaluation. The carrier frequency is set at 14 GHz with a bandwidth of 1 MHz, and the modulation scheme employed is 4QAM. The ground station gain is configured at 40 dBi to enhance the transmission capabilities, while the satellite gain is set to 30 dBi. The transmission power is fixed at 100 W, and the noise temperature is maintained at 290 K [17] to simulate typical thermal noise conditions in GEO. The jamming power introduced by the attacker is also set at 100 W. For spatial coverage, 5,000 different attacker positions are evaluated within the simulation, and 200 samples are generated for each configuration to ensure robust analysis. The radius of the VOI is specified as 5,000 km, capturing a critical area for assessing the impact of jamming nearby. The simulation parameters used in this study are summarized in Table I. In what follows, we present the performance results for the stationary and time-variant jamming models.

TABLE I: Simulation parameters

| Parameter | Value |
|------------------------------|-------|
| Frequency (GHz) | 14 |
| Bandwidth (MHz) | 1 |
| Modulation | 4QAM |
| Ground Station Gain (dBi) | 40 |
| Satellite Gain (dBi) | 30 |
| Transmission Power (W) | 100 |
| Noise Temperature (K) | 290 |
| Jamming Power (W) | 100 |
| Number of attacker positions | 5000 |
| Number of samples | 200 |
| VOI Radius (km) | 5000 |

TABLE II: Performance evaluation of random forest model without PCA

| Class | Non-jammed | Jammed |
|-------------------|------------|--------|
| Training Set Size | 2191 | 1809 |
| Testing Set Size | 547 | 453 |
| Precision (%) | 70.0 | 71.0 |
| Recall (%) | 80.0 | 59.0 |
| F1 Score (%) | 75.0 | 65.0 |
| Accuracy (%) | 70.6 | |

A. Stationary Model

Fig. 5 presents the feature selection and a comparative analysis of the confusion matrices with and without PCA. Subfigure (a) shows the correlation matrix of selected features, highlighting notable correlations such as the perfect correlation between the *total_received_power* and *rss* and the strong negative correlation between *snr_at_target* and *is_jammed*, which indicates that these features may significantly impact jamming detection accuracy. The selected features for the subsequent model training are *rss*, *distance_to_target*, *total_received_power*, *total_amplitude_mean*, *total_amplitude_std*, *total_phase_variance*. Subfigures (b)

TABLE III: Performance evaluation of random forest model with PCA

| Class | Non-jammed | Jammed |
|-------------------|------------|--------|
| Training Set Size | 2191 | 1809 |
| Testing Set Size | 547 | 453 |
| Precision (%) | 93.0 | 94.0 |
| Recall (%) | 95.0 | 91.0 |
| F1 Score (%) | 94.0 | 92.0 |
| Accuracy (%) | 93.0 | |

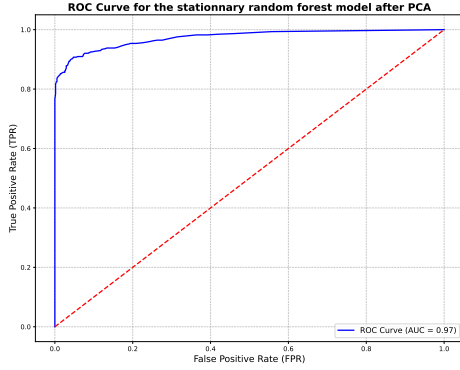


Fig. 6: ROC curve for the random forest model in the stationary scenario after applying PCA

and (c) display the confusion matrices of the random forest model without and with PCA, respectively. The confusion matrices in (b) and (c) demonstrate the impact of PCA on the random forest model’s performance for jamming detection. Without PCA (subfigure b), the model misclassifies 294 instances (110 false positives and 184 false negatives), achieving an accuracy of 70.6% as shown in Table II. With PCA applied and reduced to one dimension (Figure c), the misclassifications are significantly reduced to 70 instances (28 false positives and 42 false negatives), resulting in a much higher accuracy of 93.0% as demonstrated in Table III, indicating improved model efficiency with dimensionality reduction. This demonstrates that PCA effectively enhances model performance by focusing on the most informative features and minimizing noise.

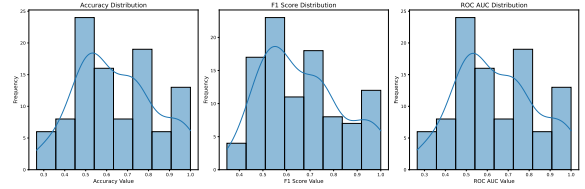
The receiver operating characteristic (ROC) in Fig. 6 demonstrates the performance of the random forest model in a stationary context after applying PCA. The blue line represents the model’s true positive rate (TPR) against the false positive rate (FPR) across different threshold values. The ROC curve’s high position near the top-left corner indicates strong classification performance, with an AUC (area under the curve) of 0.97, which signifies the excellent ability to distinguish between jammed and non-jammed states. The high AUC implies that applying PCA effectively improved the model’s classification accuracy by focusing on key features.

B. Time-Variant Model

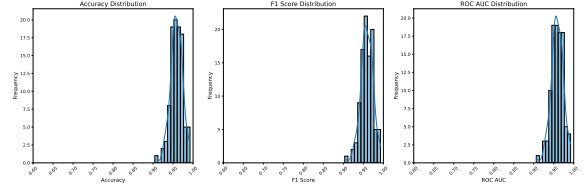
In this section, we first explore the performance of the stationary-trained random forest model with PCA presented in subsection V-A. We applied this model to the time-variant

TABLE IV: Overall performance metrics across all trajectories for the stationary trained random forest model (with PCA)

| Metric | Value (\pm Standard Deviation) |
|--------------|-----------------------------------|
| Accuracy (%) | 64.00 \pm 19.00 |
| F1 Score (%) | 66.00 \pm 17.00 |



(a) Stationary trained random forest with PCA: Accuracy, Precision, Recall



(b) Adaptive threshold technique on the time-variant dataset: Accuracy, Precision, Recall

Fig. 7: Time-variant comparison of performance metrics distribution for two methods over 100 generated trajectories on the time-variant dataset. (a) stationary trained random forest model with PCA (b) adaptive threshold technique

Normalized Confusion Matrix across predictions for multiple trajectories

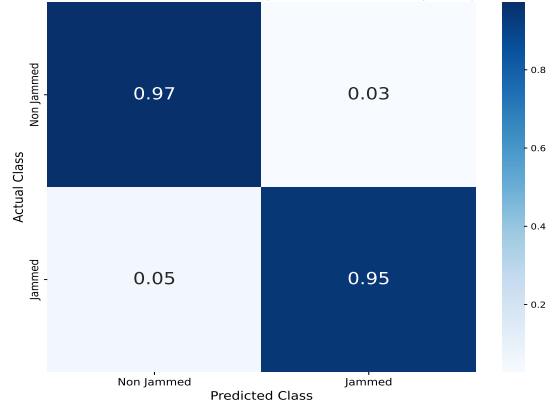


Fig. 8: Confusion matrix for the adaptive thresholding approach in the time-variant model

data to predict jamming instances. However, as indicated by the performance metrics shown in Table IV, the model significantly underperformed. The overall accuracy of 64.00% (\pm 19.00) and F1 Score of 66.00% (\pm 17.00), both with high standard deviations, suggest that the model consistently fails to perform well across different trajectories.

A key issue with this model is the considerable variability

TABLE V: Performance evaluation of the adaptive threshold approach for the time-variant model

| Class | Non-jammed | Jammed |
|-------------------------|------------|--------|
| Total Prediction Points | 25,890 | 26,394 |
| Precision (%) | 94.62 | 97.20 |
| Recall (%) | 97.23 | 94.57 |
| F1 Score (%) | 95.90 | 95.87 |
| Accuracy (%) | 95.89 | |

in its metrics across different trajectories, as seen in Fig. 7a. The large standard deviations show that the performance is highly inconsistent, which can be attributed to the different conditions present in each trajectory, such as the relative distances: the rate of change in the relative distance between the two satellites is influenced by the specific characteristics of the generated trajectories, resulting in varying dynamics of separation and approach, causing the model to perform poorly when these particular conditions arise. This inconsistency further emphasizes that the random forest model, trained on a stationary dataset, struggles to adapt to the dynamic changes in the time-variant conditions.

In contrast, in the time-variant model analysis, Fig. 8 presents a normalized confusion matrix, and Table V provides detailed performance metrics for the adaptive thresholding approach. The confusion matrix indicates high classification accuracy, with 97% of non-jammed instances and 95% of jammed instances correctly classified. Misclassification rates are low, with only 3% of non-jammed and 5% of jammed instances incorrectly classified.

Table V further supports these results by showing high precision, recall, and F1 scores for both classes, with values above 94% across all metrics. The overall accuracy of 95.89% reflects the model's robustness in adapting to time-variant conditions, effectively distinguishing between jammed and non-jammed states despite dynamic environmental changes. This high accuracy and balanced performance across metrics demonstrate that the adaptive thresholding approach performs well in the time-variant context.

VI. CONCLUSION

In this paper, we introduced a novel scenario for space-based attacks in GEO, where an illegitimate GEO satellite performs active jamming on a satellite-to-ground communication link. We explored two jamming models: a stationary model, in which the attacker remains fixed, and a time-variant model, in which the attacker follows a designated trajectory over time. We developed two distinct detection methods to detect these threats: a random forest-based algorithm enhanced with PCA for improved accuracy in the stationary model and an adaptive thresholding approach tailored to the time-variant model. Our methodology emphasizes the integration of orbital dynamics, incorporating physical constraints from satellite dynamics to enhance detection accuracy and model robustness. Simulation results demonstrate the effectiveness of these methods, achieving high accuracy in identifying both static and dynamic jamming activities and highlighting the

robustness of our detection strategies in addressing evolving jamming threats in GEO.

Future work could expand upon the current solution by incorporating a more advanced physics-informed AI model, which integrates physical principles directly into the detection algorithms. Further exploration of hybrid models that blend adaptive thresholding with machine learning could provide versatile detection capabilities across varied orbital scenarios. Finally, developing collaborative satellite networks for shared detection data and implementing proactive countermeasures are promising directions for strengthening GEO satellite link security against sophisticated on-orbit threats.

REFERENCES

- [1] H. Al-Hraishawi, H. Chougrani, S. Kisseleff, E. Lagunas, and S. Chatzinotas, "A survey on nongeostationary satellite systems: The communication perspective," *IEEE Communications Surveys & Tutorials*, vol. 25, no. 1, pp. 101–132, 2022.
- [2] C. Jiang, X. Wang, J. Wang, H.-H. Chen, and Y. Ren, "Security in space information networks," *IEEE communications magazine*, vol. 53, no. 8, pp. 82–88, 2015.
- [3] CyberPeace Institute, "Case Study: Viasat," <https://cyberconflicts.cyberpeaceinstitute.org/law-and-policy/cases/viasat>, 2022, accessed: 2024-11-1.
- [4] Y. Zhang, C. Han, F. Chu, W. Xiong, and L. Jia, "Jamming analysis between non-cooperative mega-constellations based on satellite network capacity," *Electronics*, vol. 13, no. 12, p. 2330, 2024.
- [5] N. Benchoubane, B. Donmez, O. Ben Yahia, and G. Karabulut Kurt, "Securing cislunar missions: A location-based authentication approach," in *Security for Space Systems (3S)*, 2024, pp. 1–8.
- [6] R. Han, L. Bai, C. Jiang, J. Liu, and J. Choi, "A secure architecture of relay-aided space information networks," *IEEE Network*, vol. 35, no. 4, pp. 88–94, 2021.
- [7] M. Lichtman and J. H. Reed, "Analysis of reactive jamming against satellite communications," *International Journal of Satellite Communications and Networking*, vol. 34, no. 2, pp. 195–210, 2016.
- [8] G. Taricco and N. Alagha, "On jamming detection methods for satellite Internet of Things networks," *International Journal of Satellite Communications and Networking*, vol. 40, no. 3, pp. 177–190, 2022.
- [9] U. Planta, J. Rederlechner, G. Marra, and A. Abbasi, "Let me do it for you: On the feasibility of inter-satellite friendly jamming," in *2024 Security for Space Systems (3S)*, 2024, pp. 1–6.
- [10] C. Han, A. Liu, H. Wang, L. Huo, and X. Liang, "Dynamic anti-jamming coalition for satellite-enabled army IoT: A distributed game approach," *IEEE Internet of Things Journal*, vol. 7, no. 11, pp. 10932–10944, 2020.
- [11] C. Tang, J. Ding, and L. Zhang, "LEO satellite downlink distributed jamming optimization method using a non-dominated sorting genetic algorithm," *Remote Sensing*, vol. 16, no. 6, p. 1006, 2024.
- [12] A. K and V. S, "Jamming attack detection using machine learning algorithms in wireless network," *International Journal of Advanced Research in Science, Communication and Technology (IJARSCT)*, vol. 2, no. 1, pp. 1–8, August 2022. [Online]. Available: <https://www.ijarsct.com>
- [13] A. Shafique, A. Mehmood, and M. Elhadeef, "Detecting signal spoofing attack in UAVs using machine learning models," *IEEE Access*, vol. 9, pp. 93 803–93 815, 2021.
- [14] G. Aissou, H. O. Slimane, S. Benouadah, and N. Kaabouch, "Tree-based supervised machine learning models for detecting GPS spoofing attacks on UAS," in *Ubiquitous Computing, Electronics & Mobile Communication Conference (UEMCON)*, 2021, pp. 0649–0653.
- [15] C. A. Hofmann and A. Knopp, "Satellite downlink jamming propagation measurements at ku-band," in *IEEE Military Communications Conference (MILCOM)*, 2018, pp. 853–858.
- [16] B. Garino and J. Gibson, "Space system threats," in *Space System Threats*. USAF, 2009, ch. 21, pp. 273–281.
- [17] J. Plante and B. Lee, "Environmental conditions for space flight hardware: A survey," <https://ntrs.nasa.gov/citations/20060013394>, 2005, accessed: 2024-11-13.